

Supplementary Materials for

Deconstruction of an African folk medicine uncovers a novel molecular strategy for therapeutic potassium channel activation

Angele M. De Silva, Rían W. Manville*, Geoffrey W. Abbott*

*Corresponding author. Email: abbottg@uci.edu (G.W.A.); rmanvill@uci.edu (R.W.M.)

Published 14 November 2018, *Sci. Adv.* **4**, eaav0824 (2018)

DOI: 10.1126/sciadv.aav0824

This PDF file includes:

- Fig. S1. Effects of CPT1 on KCNQ1 channels.
- Fig. S2. Effects of MTX on KCNQ1 channels.
- Fig. S3. Effects of MTX on KCNQ1/KCNE1 channels.
- Fig. S4. Effects of MTX on KCNQ1/SMIT1 channels.
- Fig. S5. Interaction of MTX with permeant ions and UCL2077.
- Fig. S6. MTX and CPT1 bind to R243 on the KCNQ1 S4-S5 linker.
- Fig. S7. Effects of MTX on KCNQ2/KCNQ3 channels.
- Fig. S8. Effects of MTX on KCNQ2-R213A/KCNQ3 channels.
- Fig. S9. Effects of MTX on KCNQ2/KCNQ3-R242A channels.
- Fig. S10. Effects of MTX on KCNQ2-R213A/KCNQ3-R242A channels.

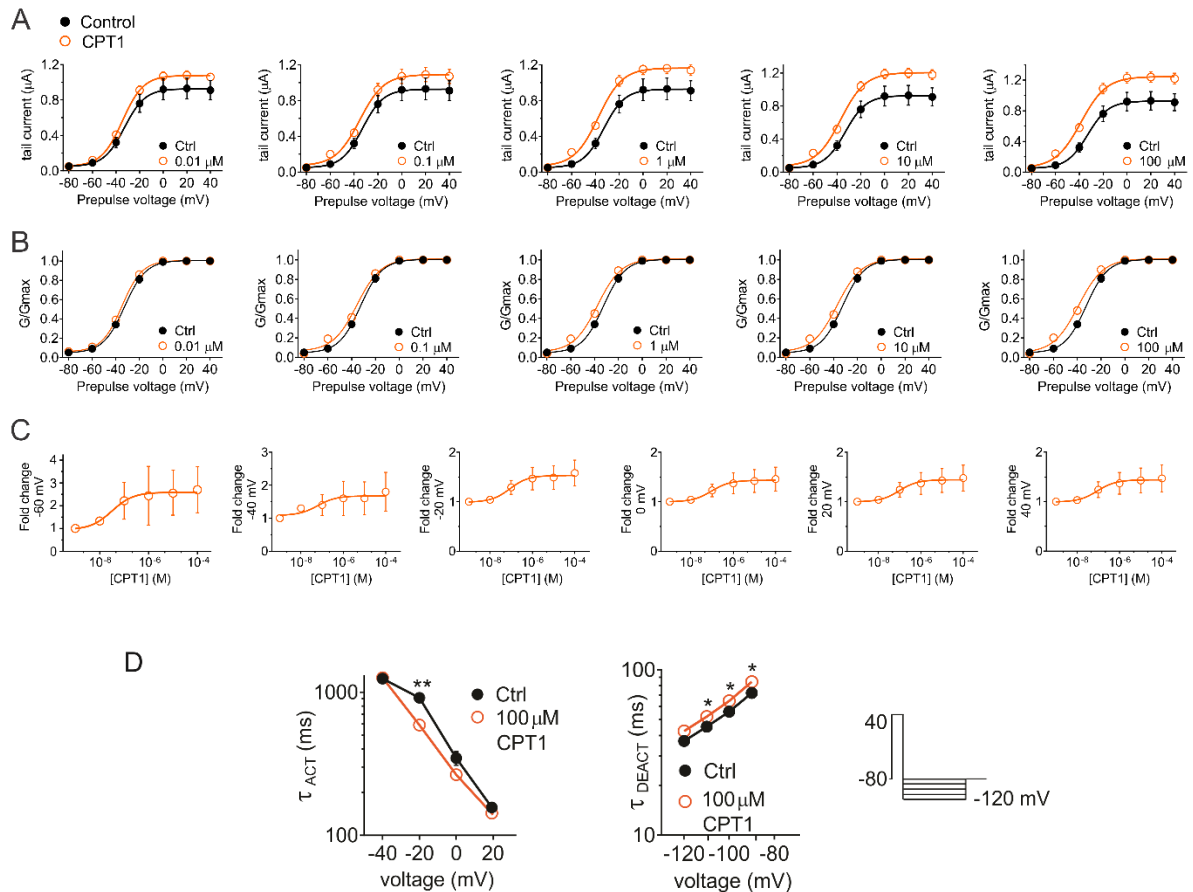


Fig. S1. Effects of CPT1 on KCNQ1 channels. (A) Mean tail current versus prepulse voltage relationship for KCNQ1 channels in the absence (black) and presence (orange) of CPT1, $n = 4-6$. (B) Normalized tail current versus prepulse voltage relationships as in panel A, $n = 4-6$. (C) Dose response of KCNQ1 channels between -40 and $+40$ mV, $n = 4-6$. Error bars indicate SEM. (D) Mean activation (*left*) and deactivation (*right*) rates versus voltage for KCNQ1 before (Ctrl) and after wash-in of CPT1 ($100 \mu\text{M}$) ($n = 6-7$; * $P < 0.05$; ** $P < 0.01$). Activation rate was quantified using voltage protocol as in Fig. 1D. Deactivation rate was quantified using voltage protocol shown on right.

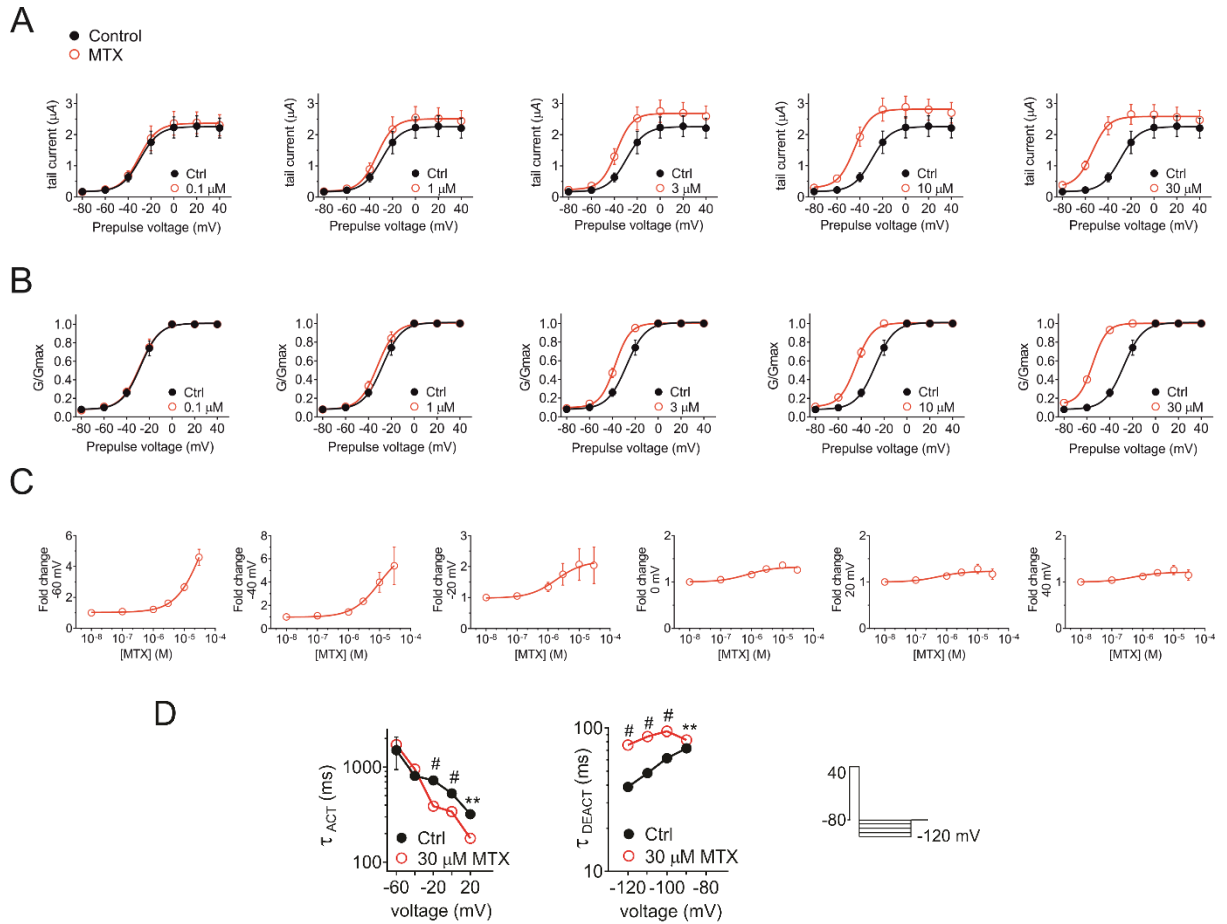


Fig. S2. Effects of MTX on KCNQ1 channels. (A) Mean tail current versus prepulse voltage relationship for KCNQ1 channels in the absence (black) and presence (red) of MTX, $n = 7$. (B) Normalized tail current versus prepulse voltage relationships as in panel A, $n = 7$. (C) Dose response of KCNQ1 channels between -40 and $+40$ mV, $n = 7$. Error bars indicate SEM. (D) Mean activation (*left*) and deactivation (*right*) rates versus voltage for KCNQ1 before (Ctrl) and after wash-in of MTX ($30 \mu\text{M}$) ($n = 7$; * $P < 0.05$; ** $P < 0.01$; # $P < 0.0001$). Activation rate was quantified using voltage protocol as in Fig. 1D. Deactivation rate was quantified using voltage protocol shown on right.

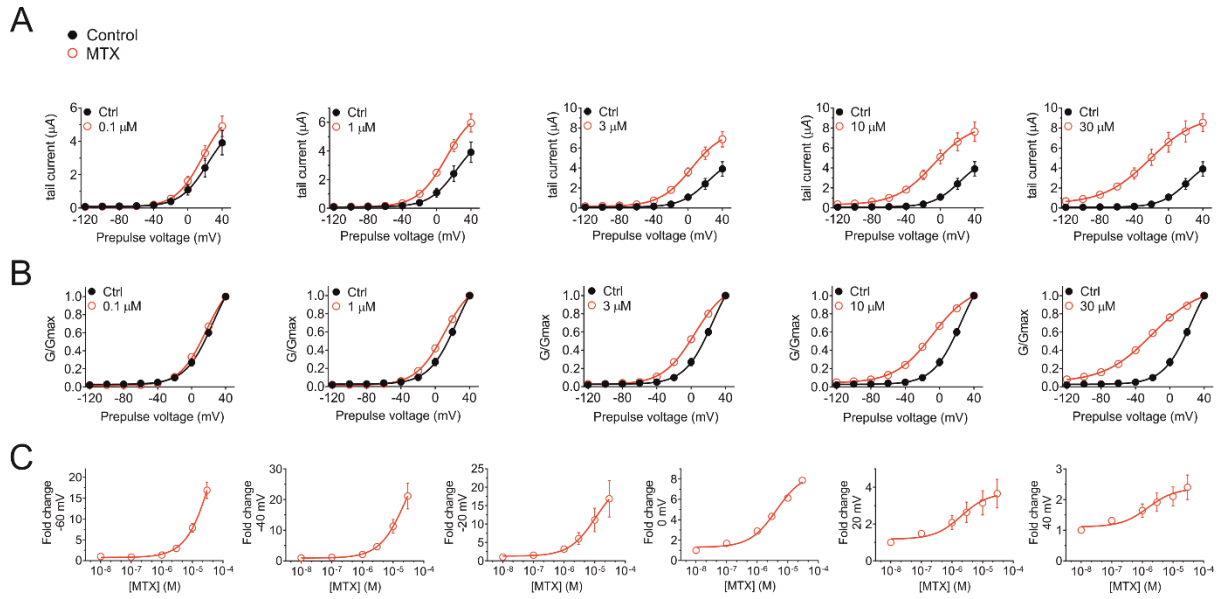


Fig. S3. Effects of MTX on KCNQ1/KCNE1 channels. (A) Mean tail current versus prepulse voltage relationship for KCNQ1/KCNE1 channels in the absence (black) and presence (red) of MTX, $n = 5$. **(B)** Normalized tail current versus prepulse voltage relationships as in panel A, $n = 5$. **(C)** Dose response of KCNQ1/KCNE1 channels between -40 and $+40$ mV, $n = 5$. Error bars indicate SEM.

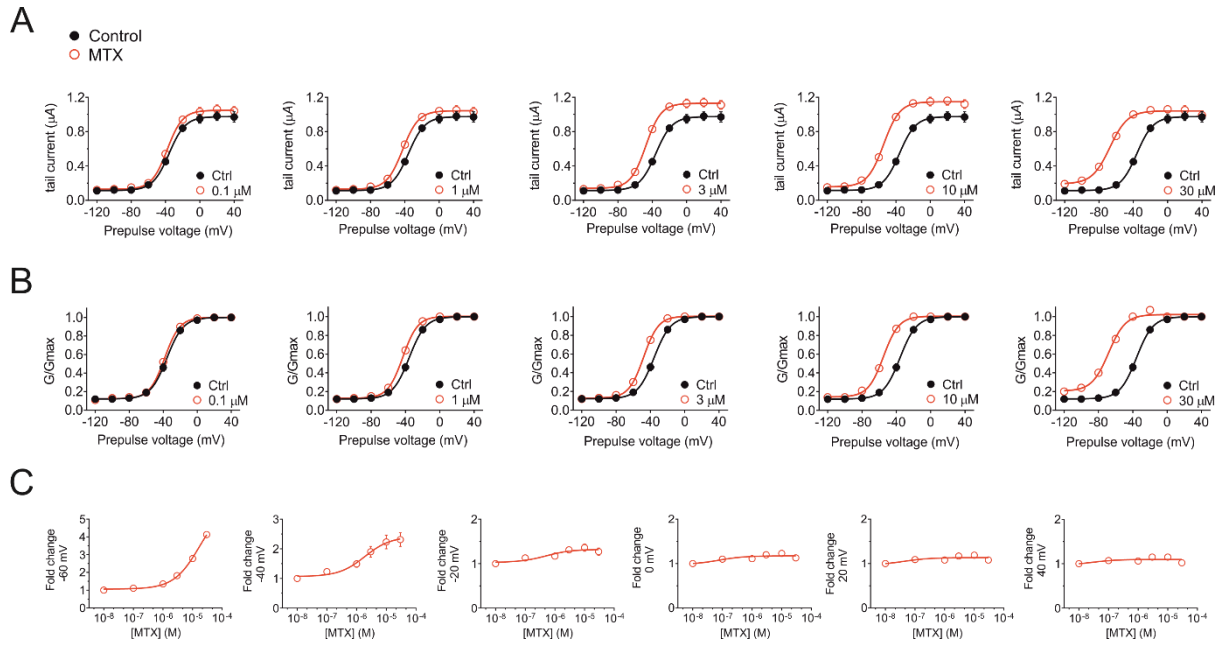


Fig. S4. Effects of MTX on KCNQ1/SMIT1 channels. (A) Mean tail current versus prepulse voltage relationship for KCNQ1/SMIT1 channels in the absence (black) and presence (red) of MTX, $n = 5$. **(B)** Normalized tail current versus prepulse voltage relationships as in panel A, $n = 5$. **(C)** Dose response of KCNQ1/SMIT1 channels between -40 and $+40$ mV, $n = 5$. Error bars indicate SEM.

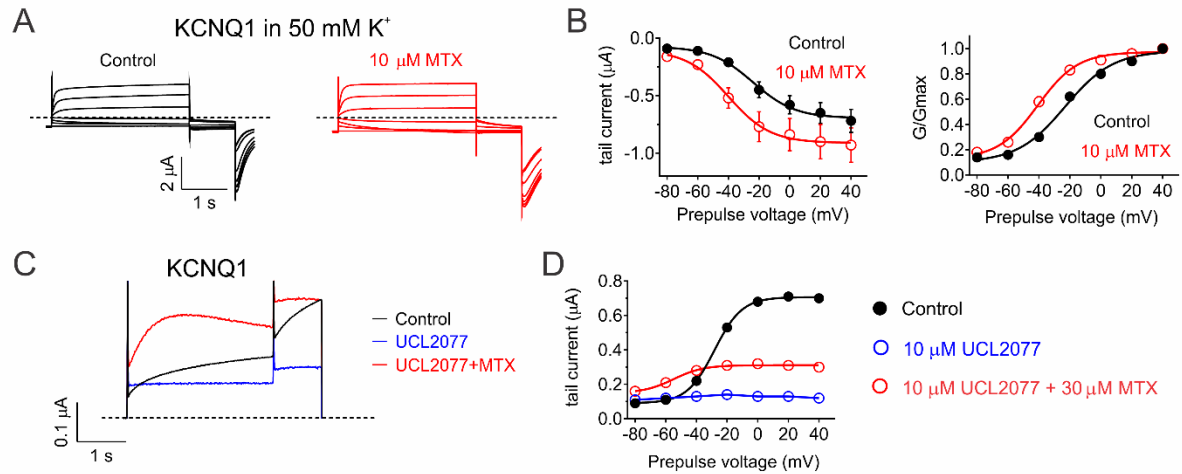


Fig. S5. Interaction of MTX with permeant ions and UCL2077.

All error bars indicate SEM. **(A)**. Averaged KCNQ1 traces with 50 mM bath K⁺ in the absence (Control) or presence of 10 μM MTX ($n = 7$). Dashed line indicates zero current level in this and all following current traces. **(B)**. Mean effects of 10 μM MTX in 50 mM bath K⁺ on KCNQ1 raw tail currents at -30 mV after prepulses as indicated (*left*) and G/G_{max} (*right*) (from traces as in A; $n = 7$). **(C)**. Averaged KCNQ1 traces, in the absence (Control) or presence of UCL2077 (10 μM) alone or with 30 μM MTX ($n = 6-11$). Cells were held at -80 mV, pulsed to -40 mV for 3 s, followed by a -30 mV tail pulse (1 s). **(D)**. Mean KCNQ1 raw tail currents at -30 mV after prepulses as indicated, in the absence (Control) or presence of UCL2077 (10 μM) alone or with 30 μM MTX (from traces as in C; $n = 6-11$).

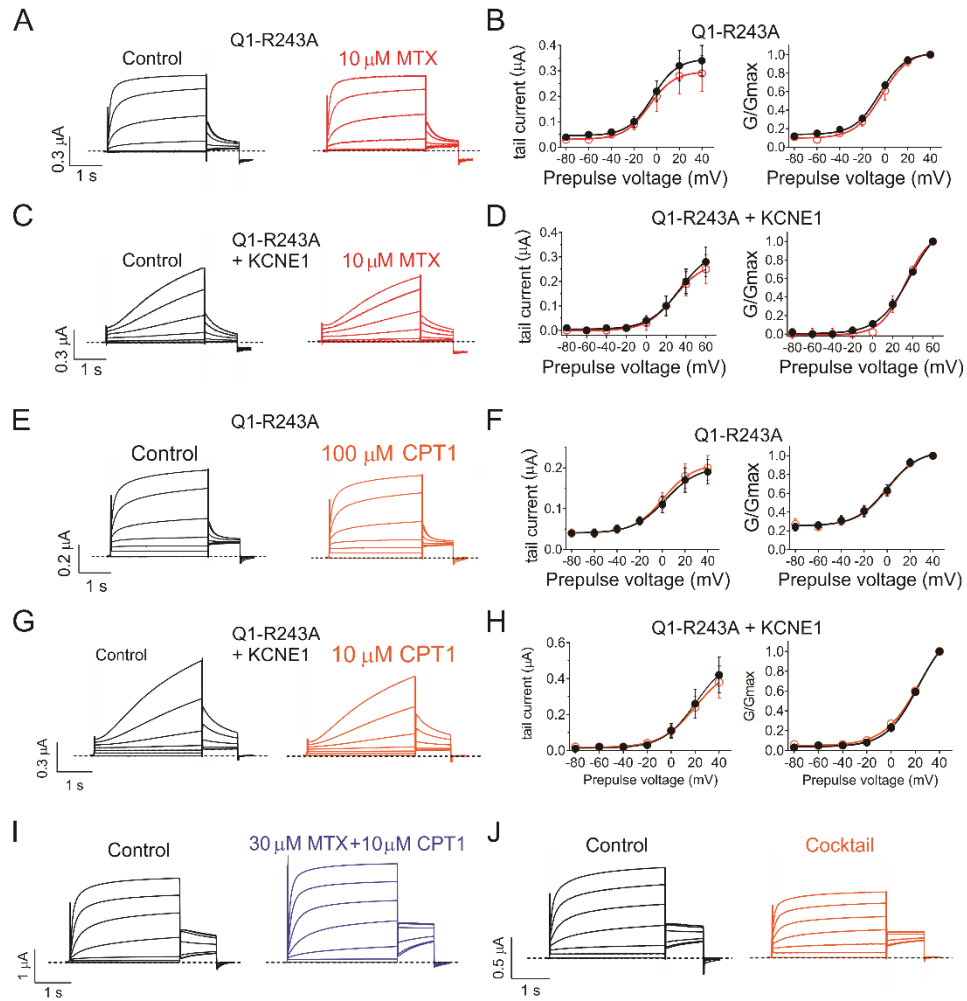


Fig. S6. MTX and CPT1 bind to R243 on the KCNQ1 S4-S5 linker. All error bars indicate SEM. **(A).** Averaged KCNQ1-R243A traces in the absence (Control) or presence of 10 μM MTX ($n = 8$). Dashed line indicates zero current level in this and all following current traces. **(B).** Mean effects of 10 μM MTX on KCNQ1-R243A raw tail currents at -30 mV after prepulses as indicated (*left*) and G/G_{max} (*right*). **(C).** Averaged KCNQ1-R243A/KCNE1 traces in the absence (Control) or presence of 10 μM MTX ($n = 5$). **(D).** Mean effects of 10 μM MTX (from traces as in **C**; $n = 5$) on KCNQ1-R243A/KCNE1 raw tail currents at -30 mV after prepulses as indicated (*left*) and G/G_{max} (*right*). **(E).** Averaged KCNQ1-R243A traces in the absence (Control) or presence of 100 μM CPT1 ($n = 10$). **(F).** Mean effects of 100 μM CPT1 (as in **E**; $n = 10$) on KCNQ1-R243A raw tail currents at -30 mV after prepulses as indicated (*left*) and G/G_{max} (*right*). **(G).** Averaged KCNQ1-R243A/KCNE1 traces in the absence (Control) or presence of 100 μM CPT1 ($n = 5$). **(H).** Mean effects of 100 μM CPT1 (as in **G**; $n = 5$) on KCNQ1-R243A/KCNE1 raw tail currents (*left*) and G/G_{max} (*right*) at -30 mV after prepulses as indicated. **(I).** Averaged KCNQ1 traces in the absence (Control) or presence of 30 μM MTX + 10 μM CPT1 ($n = 5$). **(J).** Averaged KCNQ1 traces in the absence (Control) or presence of *M. oppositifolius* leaf extract cocktail ($n = 6$).

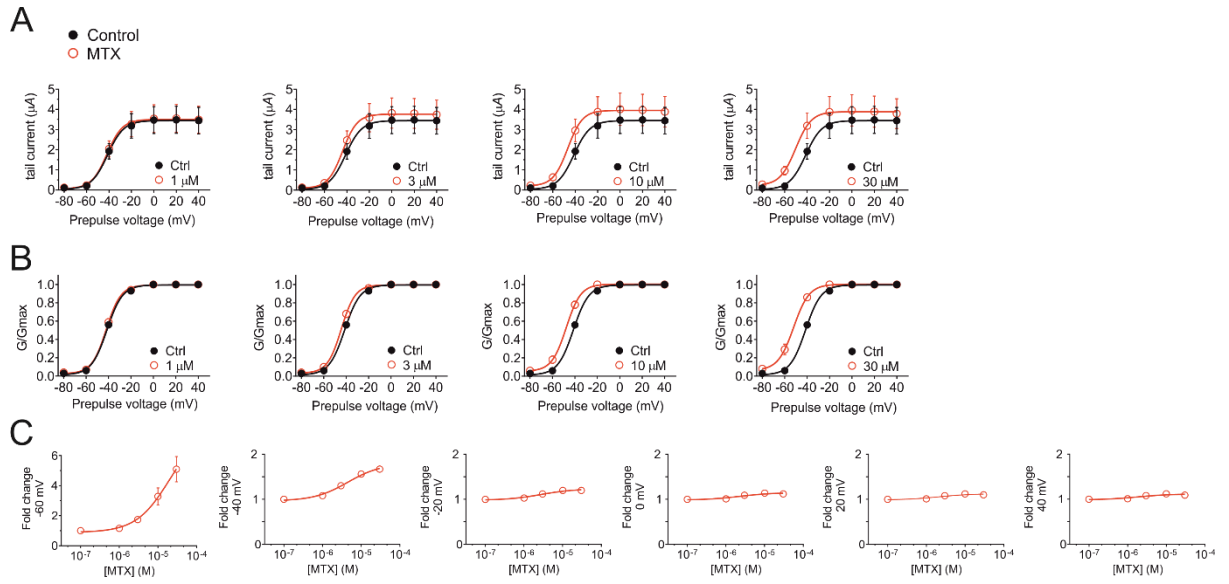


Fig. S7. Effects of MTX on KCNQ2/KCNQ3 channels. (A) Mean tail current versus prepulse voltage relationship for KCNQ2/KCNQ3 channels in the absence (black) and presence (red) of MTX, $n = 5$. (B) Normalized tail current versus prepulse voltage relationships as in panel A, $n = 5$. (C) Dose response of KCNQ2/KCNQ3 channels between -40 and $+40$ mV, $n = 5$. Error bars indicate SEM.

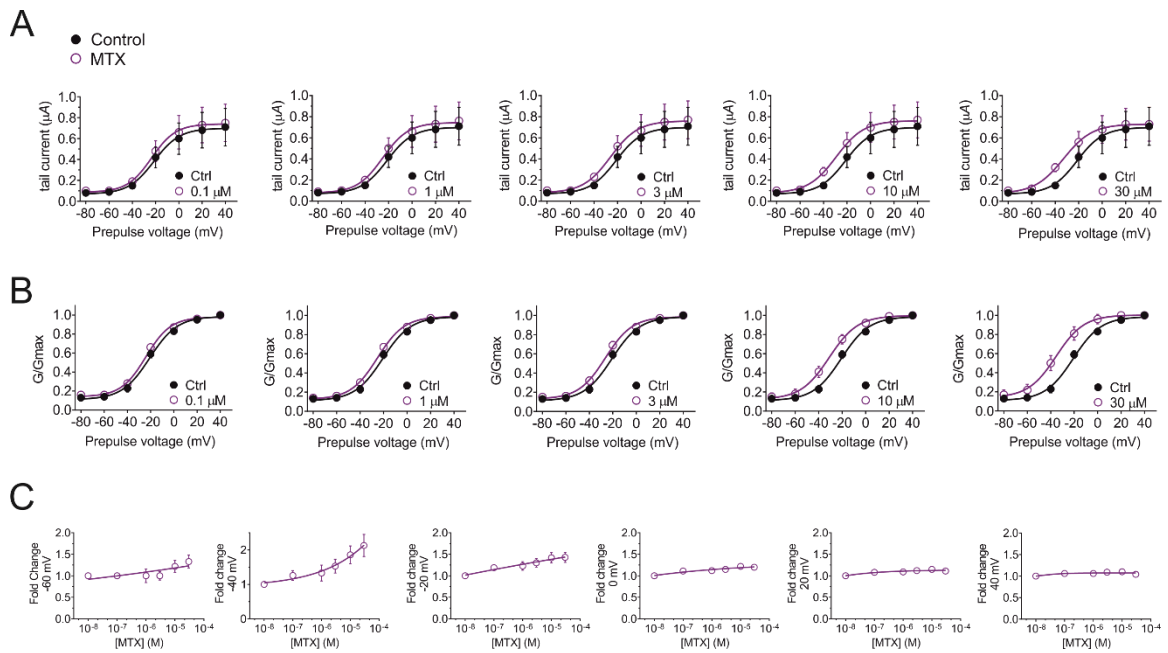


Fig. S8. Effects of MTX on KCNQ2-R213A/KCNQ3 channels. (A) Mean tail current versus prepulse voltage relationship for KCNQ2-R213A/KCNQ3 channels in the absence (black) and presence (red) of MTX, $n = 6$. (B) Normalized tail current versus prepulse voltage relationships as in panel A, $n = 6$. (C) Dose response of KCNQ2-R213A/KCNQ3 channels between -40 and $+40$ mV, $n = 6$. Error bars indicate SEM.

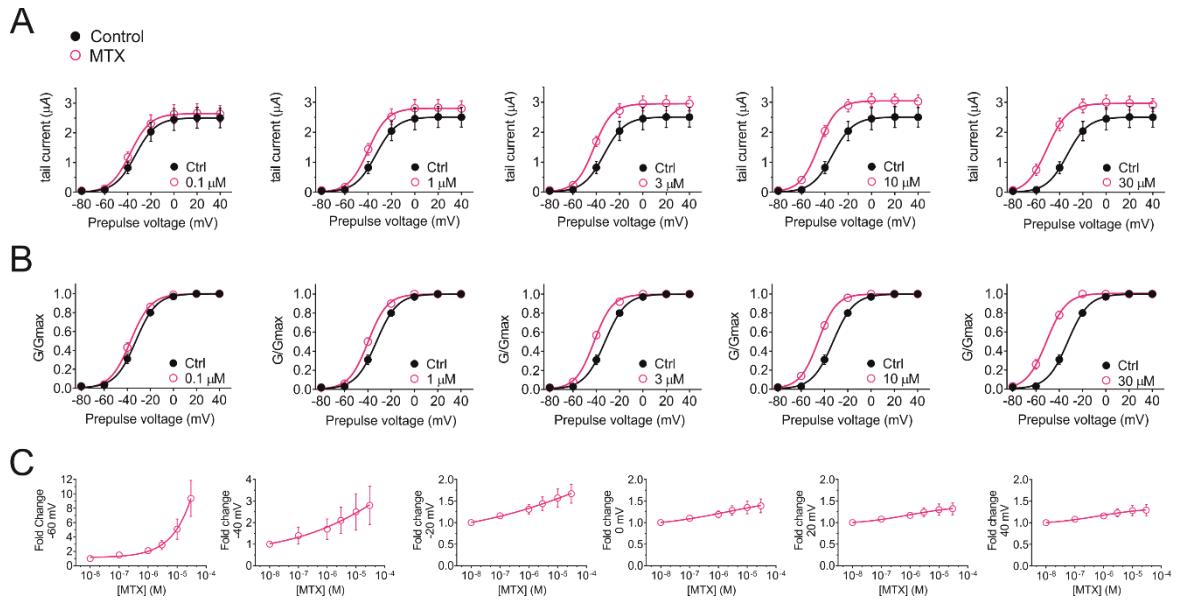


Fig. S9. Effects of MTX on KCNQ2/KCNQ3-R242A channels. (A) Mean tail current versus prepulse voltage relationship for KCNQ2/KCNQ3-R242A channels in the absence (black) and presence (red) of MTX, $n = 6$. **(B)** Normalized tail current versus prepulse voltage relationships as in panel A, $n = 6$. **(C)** Dose response of KCNQ2/KCNQ3-R242A channels between -40 and $+40$ mV, $n = 6$. Error bars indicate SEM.

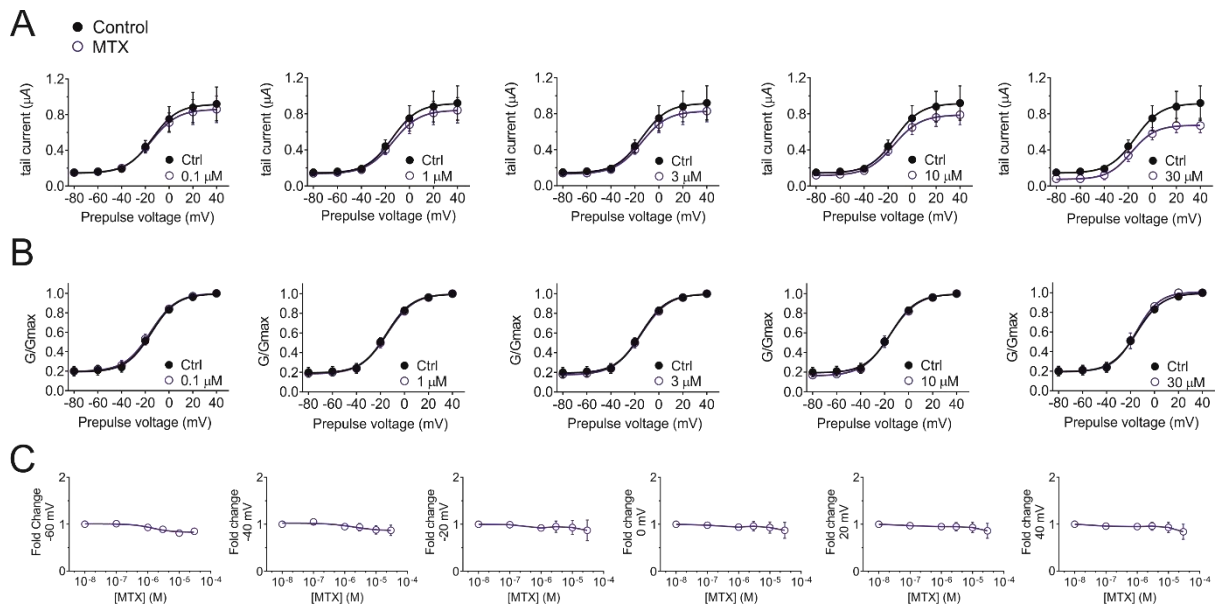


Fig. S10. Effects of MTX on KCNQ2-R213A/KCNQ3-R242A channels. (A) Mean tail current versus prepulse voltage relationship for KCNQ2-R213A/KCNQ3-R242A channels in the absence (black) and presence (red) of MTX, $n = 5$. **(B)** Normalized tail current versus prepulse voltage relationships as in panel A, $n = 5$. **(C)** Dose response of KCNQ2-R213A/KCNQ3-R242A channels between -40 and $+40$ mV, $n = 5$. Error bars indicate SEM.